Heliyon 9 (2023) e18491

Contents lists available at ScienceDirect

Heliyon

journal homepage: www.cell.com/heliyon

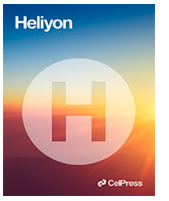

GLP-1 plays a protective role in hippocampal neuronal cells by activating cAMP-CREB-BDNF signaling pathway against CORT+HG-induced toxicity

Qi Ma [a,1], Li Wang [a,1], Xiang-Xin Liu [b,c,1], Zhi-Guo An [d], Xiao Luo [d], Li-Li Zhang [d], Ping Yan [d], Lu Jin [d], Ren Cai [e], Qi-Zhong Yi [d,f,*]

[a] *State Key Laboratory of Pathogenesis, Prevention, and Treatment of High Incidence Diseases in Central Asia, Clinical Medical Research Institute, The First Affiliated Hospital of Xinjiang Medical University, Urumqi, 830054, China*
[b] *Guangdong Mental Health Center, Guangdong Provincial People's Hospital, Guangdong Academy of Medical Sciences, China*
[c] *Department of Psychological Medicine, First People's Hospital of Kashi Region, Kashi, 844000, China*
[d] *Psychological Medicine Center, The First Affiliated Hospital of Xinjiang Medical University, Urumqi, 830054, China*
[e] *Specimen Bank of Xinjiang Key Diseases, Clinical Medical Research Institute, The First Affiliated Hospital of Xinjiang Medical University, Urumqi, 830054, China*
[f] *Xinjiang Clinical Research Center for Mental Health, Urumqi, 830054, China*

ARTICLE INFO

Keywords:
Major depressive disorder
Diabetes mellitus
GLP-1
HT22
cAMP-CREB-BDNF pathway

ABSTRACT

Major depressive disorder (MDD) with diabetes mellitus (DM) significantly reduces the quality of the patient's life, and currently, there is no effective treatment. This study explored the feasibility of Glucagon-like peptide-1 (GLP-1) in treating MDD combined with DM. The protective effects of GLP-1 on mouse hippocampal neuronal cell line HT22 cultured with corticosterone (CORT) and high glucose (HG) were assessed. HT22 cells were cultured with CORT + HG to construct a cell model of MDD combined with DM. Cell viability and cell apoptosis/necrocytosis were detected by CCK-8 assay and flow cytometry/confocal laser scanning microscopy, respectively, after treatment with GLP-1. In addition, BDNF and neurotransmitter levels, lactic dehydrogenase (LDH) and glucose levels, and proteins of cAMP-CREB-BDNF signal pathway in the culture supernatants were measured through an enzyme-linked immunosorbent assay and colorimetric assays and Western blot, respectively. The ideal intervention combination to construct a cell model of MDD combined with DM was CORT 200 μM and HG 50 mM for 48 h. After treatment of 50 nM GLP-1 for 48 h, the model+50 nM GLP-1 group's apoptosis and necrocytosis rates and LDH and glucose concentrations in the culture supernatants decreased significantly compared with the model group. However, the BDNF, 5-hydroxytryptamine (5-HT), dopamine (DA), norepinephrine (NE), PKA, *p*-CREB, and *p*-Trkb concentrations in the culture supernatants increased significantly. GLP-1 functioned against CORT + HG-induced toxicity by activating the cAMP-CREB-BDNF signaling pathway in hippocampal neuronal cells.

* Corresponding author. Psychological Medicine Center, The First Affiliated Hospital of Xinjiang Medical University, Urumqi, 830054, China.
E-mail address: qizhongyi@126.com (Q.-Z. Yi).
[1] These authors contributed equally to the study.

https://doi.org/10.1016/j.heliyon.2023.e18491
Received 13 December 2022; Received in revised form 17 July 2023; Accepted 19 July 2023
Available online 22 July 2023

1. Introduction

Major depressive disorder (MDD) and diabetes mellitus (DM) are among the top 10 non-infectious diseases worldwide. DM and MDD ranks seventh and second in disability rates among all diseases, respectively, according to the 2013 Global Burden of Disease Study [1]. MDD is prevalence in 12%–27% of DM patients, twice that of non-diabetic people [2,3]. Depressive symptoms are linked to lower medication adherence in DM patients and a significantly increased risk of DM complications [4,5]. The medical cost of DM patients with MDD is 4.5 times that of patients with DM alone, causing heavy medical and economic burdens to individuals, families, and society [6].

MDD with DM is treated separately for a single disease because the interaction between drugs is unfavorable to the control of the condition. For example, tricyclic antidepressants (TCAs), monoamine oxidase inhibitors (MAOIs), and selective 5-HT reuptake inhibitors (SSRIs) may deteriorate the metabolic situation [7]. Blood glucose control can improve the treatment effect of MDD; however, antidepressant therapy alone cannot improve blood glucose in the long term. Therefore, increased use of diabetes drugs may lead to lower adherence in MDD patients [8]. DM patients with are more susceptible to developing MDD due to the psychological burden caused by their chronic illness [9]. Therefore, developing a drug that simultaneously improves depressive symptoms and lowers blood glucose is important.

Glucagon-like peptide-1 (GLP-1) is an intestinal peptide that performs central regulation through the "gut-brain" axis and is secreted by intestinal L-cells [10]. It is used to treat type 2 diabetes. GLP-1 receptor is predominantly distributed in the pancreas, stomach, duodenum, heart, kidney, and central nervous system. After activation, GLP-1 enhances insulin secretion by being glucose-dependent, inhibits glucagon secretion, delays gastric emptying, and reduces food intake through central appetite suppression, reducing the blood glucose level [11]. GLP-1 can pass through the blood-brain barrier, bind to GLP-1 receptors distributed in the hippocampus, improve learning and memory, and play a neuroprotective role [12]. This study explored the neuroprotective effect of GLP-1 through the cAMP-CREB-BDNF signal pathway in mouse hippocampal HT22 cells. The results will provide a reliable theoretical basis for treating MDD combined with DM (Fig. 1).

2. Materials and methods

2.1. Constructing cell model of MDD combined with DM

Yaji Biotechnology Co., Ltd (Shanghai, China) provided the mouse hippocampal neuronal cell line (HT22). The cells were cultured in high-glucose (HG) DMEM containing 10% FBS (No. CM-M107, Procell) in a 37 °C cell incubator at 5% CO_2 with saturated humidity. Cell passage was initiated when the cell fusion degree reached 90% to maintain the cells in the logarithmic growth phase for subsequent experiments. Cells were treated with 25, 50, and 75 mM glucose and 0, 100, and 200 μM corticosterone (CORT) concentrations at 12, 24, 48, and 72 h. The MDD combined with the DM cell model was constructed by the optimal compatibility group.

2.2. Cell viability was detected by CCK-8 assay

This study assayed cell viability using a CCK-8 kit (Beijing TransGen Biotech Co., Ltd., Cell Counting Kit CCK, China). After trypsinization, the log phase cells were plated in a 96-well plate at 5000 cells/well. The cells were incubated at 37 °C with 5% CO_2 for 24 h. The culture medium of each group was replaced with different concentrations of glucose and corticosterone, and 100 μL 10% CCK-8 solution was added to the medium at 12, 24, 48 and 72 h. After incubation for 1 h, the optical density (OD) value was

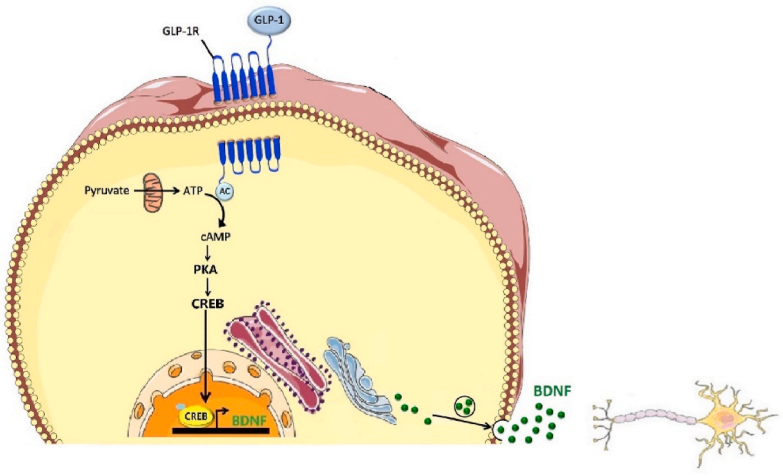

Fig. 1. GLP-1 activates the cAMP-CREP-BDNF signaling pathway by activating the GLP-1 receptor.

determined at 450 nm using a microplate meter.

2.3. Cell apoptosis was detected by flow cytometry

Cell apoptosis was assayed by the Annexin V-PE Apoptosis Detection Kit I (BD Biosciences, CAT#: 559763, USA) according to the manufacturer's instructions. Cells and medium (containing apoptotic and necrotic cells generated under cultured conditions) were collected in a centrifuge tube, centrifuged at room temperature for 5 min at 1000 rpm, and the supernatant was discarded. Cells were washed twice with prechilled PBS, and the supernatant was discarded. Next, 500 μL 1 × Binding Buffer was added and filtered with a 0.22-μm filter to obtain the single-cell suspension. Annexin V-PE (5 μL) and 7-AAD (10 μL) were added to each tube, mixed gently, and incubated at 4 °C in the dark for 5 min. The apoptotic cells were detected within 30 min using an LSRFortessa flow cytometer (BD Biosciences, USA).

2.3.1. Necrocytosis was detected by confocal laser scanning microscopy

Necrocytosis was detected by confocal laser scanning microscopy. The cells were seeded at a concentration of 5×10^4 cells/mL in 500 μL in 24-well plates and incubated for 24 h. Cells were cultured in complete medium (control group), 50 mM HG + 200 μM CORT (model group), and 50 mM HG + 200 μM CORT + 50 nM GLP-1 (intervention group) for 48 h. Then the media were discarded, and the cells were washed thrice with 1 × PBS (pH = 7.4). The cells were stained with Hoechst 33342 and Propidium Iodide (PI) for 30 min at 4 °C and rinsed twice with 1 × PBS (pH = 7.4). Cells were visualized under a confocal microscope (Leica, TCS-SP5).

2.4. Measurement of BDNF and neurotransmitter levels in culture supernatants through enzyme-linked immunosorbent assay

The BDNF, and neurotransmitter levels in cell culture supernatant were quantified by ELISA kit according to the manufacturer's protocol (BDNF: Hulti Sciences (Lianke) Biotech, Co., Ltd., Hangzhou, China; 5-HT, NE, DA: Cusabio Technology Co., Ltd, Wuhan, China). The OD value was detected at 450 nm using a multi-function microplate reader (xMark™, Bio-Rad, USA).

2.5. Measurement of LDH and glucose levels in culture supernatants through colorimetric assay

The LDH was measured by Lactate Dehydrogenase Assay Kit according to the manufacturer's protocol (Nanjing Jiancheng Corp., Nanjing, China). The OD value was detected at 450 nm using a multi-function microplate reader (xMark™, Bio-Rad, USA). (Equation (1).

$$\text{LDH}\ (\text{U}/\text{L}) = \frac{\boldsymbol{sample\ OD - control\ OD}}{\boldsymbol{standard\ OD - control\ OD}} \times \text{standard concentration}\ (0.2\ \mu\text{mol}/\text{L}) \times 1000 \qquad \text{Equation (1)}$$

The glucose was measured by Glucose kit through glucose oxidase method (Nanjing Jiancheng Corp., Nanjing, China). The OD value was detected at 450 nm using a multi-function microplate reader (xMark™, Bio-Rad, USA). Equation (2).

$$\text{Glucose}\ (\text{mmol}/\text{L}) = \frac{\boldsymbol{sample\ OD - control\ OD}}{\boldsymbol{standard\ OD - control\ OD}} \times \text{standard concentration}\ (5.5\ \text{mmol}/\text{L}\ ) \qquad \text{Equation (2)}$$

2.6. Measurement of protein of cAMP-CREB-BDNF signal pathway through Western blot assay

Cells were washed with cold PBS, lysed with RIPA buffer, and kept on ice for 1 h. The protein was incubated by centrifugation at 12,000 rpm, 4 °C for 10 min, and its concentration was quantified using a Bicinchoninic Acid assay with an Easy II Protein Quantitative kit (Beijing TransGen Biotech Co., Ltd., Beijing, China). Protein samples were separated by 10% SDS-PAGE and transferred to a polyvinylidene fluoride (PVDF) membrane. The membrane was blocked with 5% nonfat milk (prepared with TBS-T) for 1 h at room temperature. Membranes were incubated overnight at 4 °C primary antibody (β-actin (Sino Biological, China; 1:1000), PKA (Abcam, USA; 1:1000), CREB (Abcam, USA; 1:1000), *p*-CREB (Abcam, USA; 1:800), Trkb (Abcam, USA; 1:1000), and *p*-Trkb (Abcam, USA; 1:800)). The membranes were washed and incubated with a secondary antibody at room temperature for 1 h. Protein expression was visualized using chemiluminescence on the Bio-Rad system.

2.7. Statistical analysis

All quantitative data were presented as the mean ± standard deviation and performed using SPSS software (version 25.0). Each experiment was repeated thrice independently. One-way ANOVA was performed to analyze the differences between groups. $P < 0.05$ was considered a statistically significan difference.

3. Results

3.1. CORT + HG treatment construct MDD combined with DM cell model

This study treated HT22 cells with nine combinations of 0, 100, and 200 μM corticosterone (CORT) and 25, 50, and 75 mM glucose

concentrations. The neuron survival rate decreased with the increase of CORT and HG concentrations. The combination of CORT 200 μM and HG 50 mM was an ideal intervention concentration because the cell survival and BDNF concentration in culture supernatants at this combination were decreased to 56.92% and 44.45%, respectively, compared with control (CORT 0 μM and HG 25 mM) in CCK-8 assay, and ELISA, respectively. In contrast, the LDH concentration in culture supernatants was elevated by 1.61-fold control (Fig. 2A–C).

This study added CORT 200 μM and HG 50 mM into the cell culture medium and detected cell survival and BDNF and LDH concentrations in culture supernatants at 12, 24, 48, and 72 h. The results showed that the intervention effect was optimal at 48 h; OD values of cell survival rate in control and model groups were 0.801 ± 0.025 and 0.441 ± 0.028, respectively, $t = 21.374$, $P < 0.001$. In addition, BDNF concentrations in culture supernatants were 140.577 ± 13.515 and 87.882 ± 8.463 ng/ml, respectively, $t = 5.724$, $P < 0.01$. Moreover, LDH concentrations in culture supernatants were 130.833 ± 31.058 and 325.00 ± 29.475 U/L, respectively, $t = -7.854$, $P < 0.01$. Therefore, HT22 cells cultured with CORT 200 μM and HG 50 mM for 48 h could construct the cell model of MDD combined with DM (Fig. 2D–F).

3.2. Optimum concentration of GLP-1

This study added 10, 20, 50, and 100 nM GLP-1 into the cell culture medium to determine the optimal intervention concentration of GLP-1. At 48 h, the morphology of HT22 cells in each group was observed and photographed under the 100 × optical microscope, the cell viability of each group and BDNF and LDH concentrations in the culture supernatant were detected by CCK8 assay, ELISA, and colorimetry, respectively. The cell count in the model group exhibited a significant reduction compared to that of the control group, which gradually increased with an elevation in GLP-1 concentration (Fig. 3A–F). Compared with the control group, the cell viability of the model and the model + GLP-1 concentrations of 10, 20, 50, and 100 nM groups decreased to 56.2%, 69.9% ($P < 0.0001$), 70.2% ($P < 0.0001$), 82.3% ($P < 0.0001$), and 91.0% ($P < 0.001$), respectively (Fig. 3G). The BDNF concentration in cell culture supernatant of control, model, model + GLP-1 concentrations of 10, 20, 50, and 100 nM groups were 131.110 ± 14.391 ng/ml, 58.247 ± 4.711 ng/ml, 108.504 ± 16.555 ng/ml, 107.538 ± 3.125 ng/ml, 135.269 ± 9.264 ng/ml, and 152.634 ± 5.758 ng/ml, respectively (Fig. 3H). The LDH concentration in cell culture supernatant of control, model, model + GLP-1 concentrations of 10, 20, 50, and 100 nM groups were 133.333 ± 15.927 U/L, 302.682 ± 28.743 U/L, 282.758 ± 33.155 U/L, 239.080 ± 30.149 U/L, 177.887 ± 12.661 U/L, and 200.766 ± 36.661 U/L, respectively (Fig. 3I). Therefore, 50 nM was the optimal intervention concentration of GLP-1.

3.3. Protective effect of GLP-1 on CORT + HG-induced apoptosis and necrosis of HT22 cells

This study performed flow cytometry and confocal laser scanning microscopy to assess the effects of GLP-1 on the apoptosis and necrosis of HT22 cells cultured under the CORT + HG conditions. Flow cytometry results showed that the apoptosis rate of the model group increased significantly than the control group. After GLP-1 treatment, the apoptosis rate decreased (Fig. 4A). Cell necrosis was observed using confocal laser scanning microscopy after Hoechst 33342 and PI staining. Since Hoechst 33342 can penetrate through cell membranes, the fluorescence intensity of apoptotic cells was significantly enhanced compared with normal cells. In contrast, PI cannot penetrate the cell membrane or stain normal or apoptotic cells with intact cell membranes. Therefore, the differential staining effect of Hoechst 33342 and PI can detect normal cells (weak red and weak blue fluorescence) and necrotic cells (strong red and strong blue fluorescence). The results showed that compared with the control group, Hoechst 33342 and PI fluorescence intensity were significantly increased in the model group. After GLP-1 (50 nM) treatment, the two-fluorescence intensity was decreased (Fig. 4B).

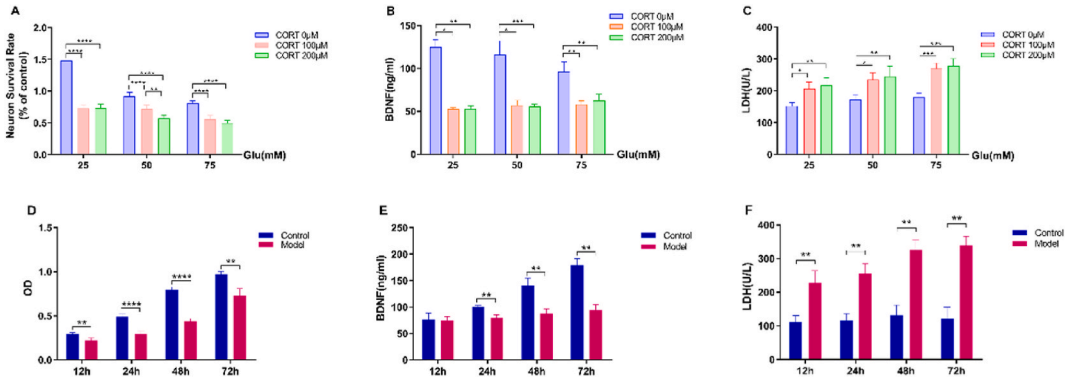

Fig. 2. The cell survival rate and BDNF and LDH concentrations in culture supernatants of HT22 cells with different CORT and HG concentrations and time. (n = 3 per group). A: The neuron survival rate of HT22 cells was measured under various concentrations of CORT and Glu; B: BDNF concentration was measured in culture supernatants under various concentrations of CORT and Glu; C: LDH concentration was measured in culture supernatants under various concentrations of CORT and Glu; D: OD values of cell survival rate were measured at different time points; E: BDNF concentration was measured in culture supernatants at different time points; F: LDH concentration was measured in culture supernatants at different time points. CORT: Corticosterone; Glu: Glucose. Control: HG 25 mM + CORT 0 μM; Model: HG 50 mM + CORT 200 μM *$P < 0.05$, **$P < 0.01$, ***$P < 0.001$, ****$P < 0.0001$.

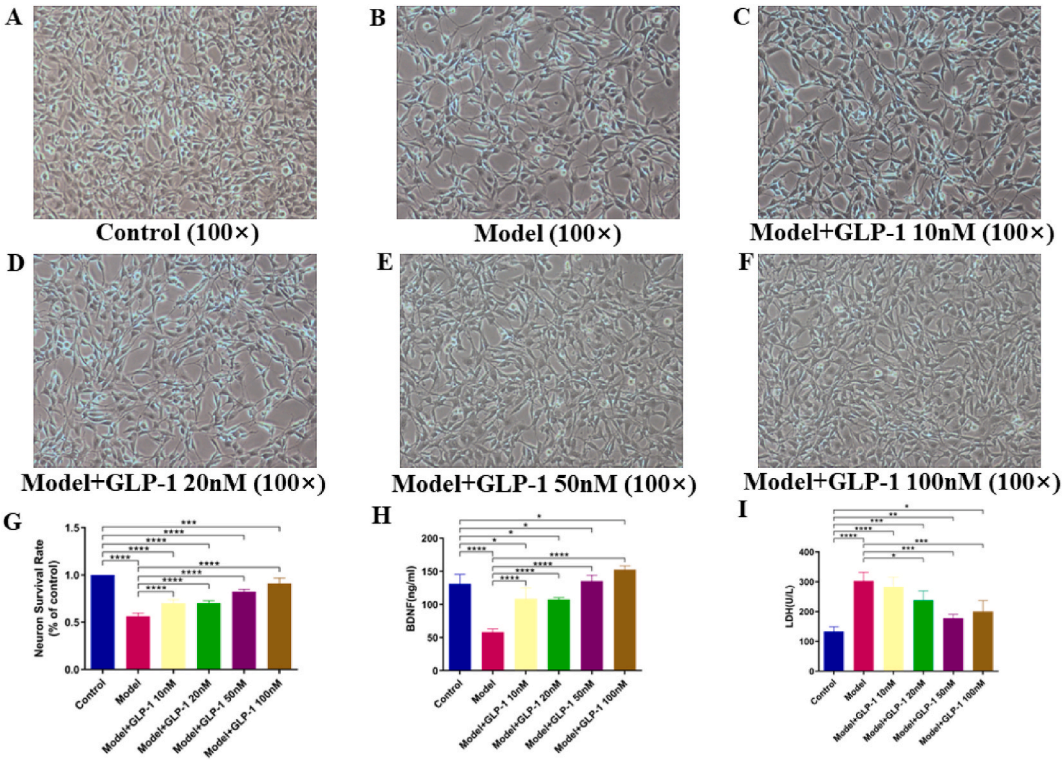

Fig. 3. Effects of different GLP-1 concentrations on HT22 cell survival rate, and BDNF and LDH concentrations in culture supernatants (n = 3 per group). A–F: The morphology of HT22 cells in each group was observed under optical microscope. Scale bar: × 100; G: The neuron survival rate of HT22 cells was measured under various concentrations of GLP-1; H: BDNF concentration was measured in culture supernatants under various concentrations of GLP-1; I: LDH concentration was measured in culture supernatants under various concentrations of GLP-1. Control: HG 25 mM + CORT 0 μM; Model: HG 50 mM + CORT 200 μM *$P < 0.05$, **$P < 0.01$, ***$P < 0.001$, ****$P < 0.0001$.

Therefore, GLP-1 treatment has a protective effect against apoptosis and necrotic of HT22 cells under the CORT + HG conditions.

3.4. Effects of GLP-1 on the neurotransmitter and glucose in the culture supernatant of HT22 cells cultured with CORT + HG

This study used the ELISA method to detect the effects of GLP-1 on the neurotransmitter of CORT + HG cultured HT22 cells. The results revealed that the concentrations of 5-HT, NE and DA in the culture supernatant of the model group were lower than that of the control group (5-HT: 2270.95 ± 83.02 *vs.* 2629.59 ± 120.33 pg/ml, $n = 3$, $P < 0.01$; NE: 41.10 ± 2.54 *vs.* 63.03 ± 9.98 pg/ml, $n = 3$, $P < 0.05$; DA: 17.80 ± 1.76 *vs.* 32.26 ± 9.07 pg/ml, $n = 3$, $P < 0.05$). After 50 nM GLP-1 treatment, the concentration of neurotransmitter increased significantly; 5-HT, NE, and DA increased to 2738.84 ± 107.09 pg/ml ($P < 0.01$), 81.64 ± 7.33 pg/ml ($P < 0.001$), and 51.72 ± 2.58 pg/ml ($P < 0.001$), respectively (Fig. 5A–C).

The glucose oxidase method was used to detect the glucose content in the supernatant. The glucose concentration in the supernatant of the model group was significantly higher than that of the control group (8.28 ± 0.53 *vs.* 4.33 ± 0.55 mmol/L, $n = 3$, $P < 0.0001$). After 50 nM GLP-1 treatment, glucose concentration decreased to 6.347 ± 0.73 mmol/L, which was statistically significant compared with the model group ($P < 0.01$) (Fig. 5D). Since the model group cells were cultured in a high glucose medium, it was reasonable that the glucose content in the supernatant was significantly increased. However, glucose concentration decreased significantly after GLP-1 intervention, suggesting that GLP-1 can effectively improve the glucose metabolism of HT22 cells.

3.4.1. GLP-1 reversed the cAMP-CREB-BDNF signaling pathway inhibition in HT22 cells caused by CORT + HG

This study used the Western blot assay to detect key members of the cAMP-CREB-BDNF signaling pathway in the HT22 cells, the target strip was consistent with the expected size (Fig. 6A; the original Western blot figure in Fig. S1). β-actin expression was used as the internal standard, and the relative PKA protein expressions in the control, model, and GLP-1 groups were 0.50 ± 0.01, 0.27 ± 0.04, and 0.473 ± 0.06, respectively (Fig. 6B). Compared with the model group, the PKA protein/β-actin ratio was the difference between the control and GLP-1 intervention groups ($P < 0.001$). The *p*-CREB/CREB ratio in the control, model, and GLP-1 groups were 0.444 ± 0.014, 0.306 ± 0.017, and 0.431 ± 0.015, respectively. Due to the CORT + HG culture, the *p*-CREB/CREB ratio was significantly lower than that in the control group ($P < 0.0001$). After treatment with 50 nM GLP-1, the ratio was comparable with the control group (Fig. 6C). Similarly, HG + CORT culture caused the *p*-TrkB/Trkb ratio in the model group to be significantly lower than that in the control group (0.35 ± 0.03 *vs.* 0.51 ± 0.09, $P < 0.05$). After treatment with 50 nM GLP-1, the *p*-TrkB/Trkb ratio increased significantly,

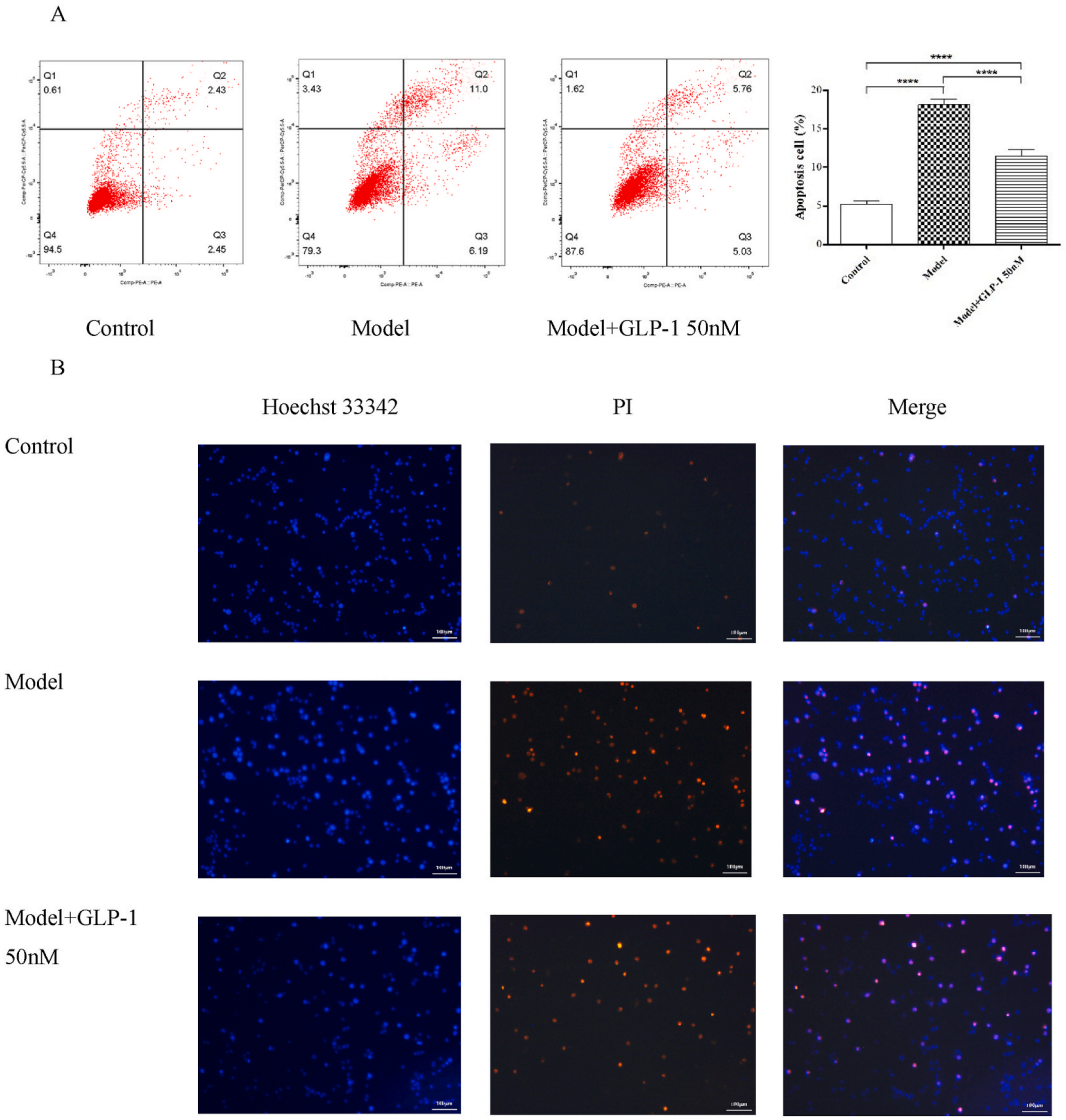

Fig. 4. Effects of GLP-1 on the HT22 cells cultured under the CORT + HG condition. (n = 3 per group). A: Detection of apoptotic cells by flow cytometry; B: Necrosis and apoptotic cells were observed under a microscope following Hoechst 33342 and PI co-staining. Scale bar: 100 μm.

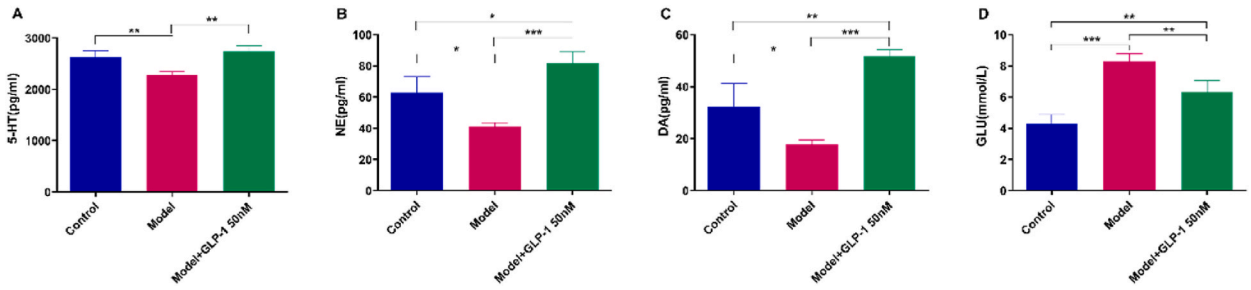

Fig. 5. Effects of GLP-1 on the neurotransmitter and glucose in the culture supernatant of HT22 cells cultured with CORT + HG ($n = 3$ per group). The ELISA method was used to detect the effects of GLP-1 on 5-HT (A), NE (B), and DA (C) of HT22 cells cultured with CORT + HG. The glucose oxidase method was used to detect the glucose content of HT22 cells in the supernatant (D). $^{*}P < 0.05$, $^{**}P < 0.01$, $^{***}P < 0.001$.

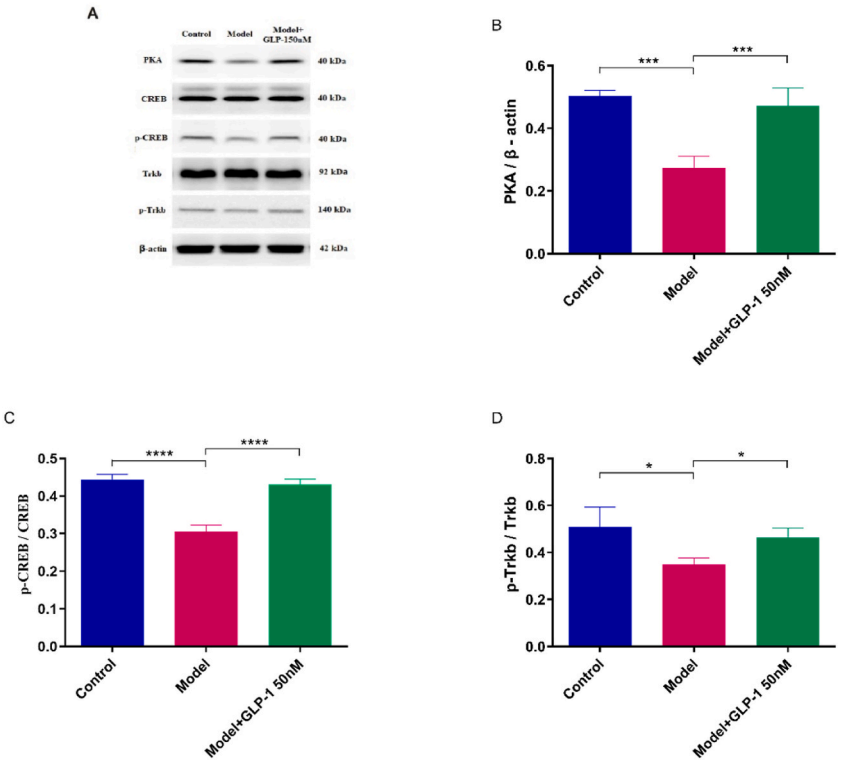

Fig. 6. Expression of key members of the cAMP-CREB-BDNF signaling pathway in the cell model of depression with combined diabetes mellitus ($n = 3$ per group). A: Representative Western blotting image (The original Western blot figure in Fig. S1). Western blotting detected the PKA, CREB, *p*-CREB, Trkb, *p*-Trkb and β-actin expression levels in HT22 cells Bar chart showing the ratios of PKA/β-actin (B), *p*-CREB/CREB (C) and *p*-Trkb/Trkb (D) in HT22 cells. $^{*}P < 0.05$, $^{***}P < 0.001$, $^{****}P < 0.0001$.

and the differences were statistically significant compared with the model group (0.46 ± 0.04 *v.s.* 0.35 ± 0.03, $P < 0.05$) (Fig. 6D). These data indicate that GLP-1 can reverse the cAMP-CREB-BDNF signaling pathway inhibition in HT22 cells caused by CORT + HG.

4. Discussion

The complex array of multidirectional linkages between MDD and DM raises the possibility of a shared etiology [13]. The hippocampus is a part of the limbic system responsible for memory and emotion processing, associated with MDD and DM. Neurogenesis is the proliferation of new neurons in the brain. Hippocampal neurogenesis-deficient mice shown symptoms of anhedonia, suggesting that the hippocampus mediates depressive symptoms [14]. MDD and DM are associated with hippocampal volume reduction [15,16]. The volume of gray matter in the hippocampus begins to decrease in the early stages of MDD in patients, and changes in other brain regions occur as the disease progresses [17]. Likewise, neuroimaging studies have demonstrated impaired functional connectivity between the left hippocampus and multiple core brain regions of the default network in DM patients [18]. Therefore, understanding the connection between MDD and DM requires an investigation of neuroplastic changes in the hippocampus. Cellular models are frequently employed alone or in conjunction with animal studies to investigate the mechanisms of depression and antidepressants [19]. Hydrogen peroxide or glucocorticoids are often used to induce primary neuronal cell models (cortical or hippocampal neurons), neuronal cell lines (rat clonal pheochromocytoma PC12, human neuroblastoma SH-SY5Y, and mouse hippocampal HT-22), primary glial cell cultures (astrocytes, microglia), and glial cell lines (rat glioma C6, microglial BV2) to construct the cell model of MDD [19,20]. This study stimulated mouse hippocampal neuronal cell line (HT22 cell) with CORT and HG to simulate hippocampal neuron damage in the comorbidity of MDD and DM. To closely replicate the real clinical situation, this study used BDNF and glucose as the evaluation indexes of MDD and DM, respectively, to verify that the model was successfully established. In addition, LDH release is related to cell membrane integrity. It can leak into cell culture supernatant when the cell membrane is damaged or the permeability of the cell membrane is increased, and the release amount is positively correlated with the degree of cell damage. Therefore, detecting LDH concentration in culture supernatant is evidence to determine cytotoxicity [21].

GLP-1 is an intestinal peptide with extensive pharmacological effects. It treats type 2 diabetes and obesity and has cardio- and neuroprotective effects. GLP-1 affects learning, memory, and reward behavior by reducing inflammation and apoptosis [12]. In addition, GLP-1 receptor agonists alleviate depressive symptoms [22]. The previous study by this study's authors found that the plasma and fecal GLP-1 levels of the MDD group were lower than those of the control group [23]. In animal experiments, GLP-1 receptor agonist liraglutide reverses the metabolic abnormalities and behavioral depression caused by the long-term administration of atypical

antipsychotics [24]. Therefore, GLP-1 could be used as a potential therapy for depression in diabetes. The original depression hypothesis suggests that the pathological basis of depression was the disorders of 5-HT, NE, and DA [25,26]. Commonly used antidepressant drugs, such as SSRIs, TCAs, and MAOIs, inhibit related transporters to increase the concentration of neurotransmitters in the brain [27]. This study observed that CORT + HG induced the cell model of MDD combined with DM, decreasing survival rate, glucose utilization, and BDNF, 5-HT, DA, and NE production abilities of HT22 cells and increasing apoptosis and necrosis. GLP-1 treatment reversed the activity of damaged HT22 cells, reduced apoptosis, necrosis, and glucose concentration, and increased BDNF, 5-HT, DA, and NE levels in the culture medium, providing more evidence for GLP-1 treatment of MDD combined with DM.

cAMP-CREB-BDNF signaling pathway is an important factor in neurogenesis and neuronal cell repair related to learning, memory, and cognitive function [28,29]. cAMP exerts its effects primarily through PKA stimulation, which phosphorylates CREB. When CREB is activated, BDNF, a powerful trophic factor that affects synaptic plasticity and neuronal shape, is produced [30,31]. MDD patients who died by suicide had reduced cAMP levels in the prefrontal cortex [28]. Postmortem studies showed that patients with significant depression had low levels of the phosphorylation level of CREB in the hippocampus [32]. In the chronic unpredictable stress animal model, CREB expression was inhibited in the hippocampal CA1 region; however, CREB levels recovered after antidepressant treatment [33]. Through modulation of cAMP-CREB-BDNF and other similar signaling pathways, numerous neuroprotective agents have been developed against neurodegenerative and neurobehavioral disorders [34]. This study observed that the PKA, *p*-CREB, and *p*-Trkb (BDNF-specific receptor) expressions were significantly increased after the GLP-1 treatment to the culture medium of HT22 cells, which were damaged by CORT + HG, suggesting that GLP-1 could up-regulate the cAMP-CREB-BDNF signaling pathway. The underlying mechanism promotes GLP-1 to exert protective effects on neuronal cells. These novel results provide new insights into the molecular role of GLP-1 in hippocampal cells. Further studies will confirm these findings and explore the feasibility of GLP-1 as a treatment for MDD combined with DM.

Author contribution statement

Qi Ma: Conceived and designed the experiments; Performed the experiments; Analyzed and interpreted the data; Wrote the paper.
Li Wang: Performed the experiments.
Xiang-Xin Liu: Contributed reagents, materials, analysis tools or data; Wrote the paper.
Zhi-Guo An: Xiao Luo: Li–Li Zhang: Ping Yan: Lu Jin: Ren Cai: Contributed reagents, materials, analysis tools or data.
Qi-Zhong Yi: Conceived and designed the experiments; Wrote the paper.

Funding statement

This study was supported by State Key Laboratory of Pathogenesis, Prevention and Treatment of High Incidence Diseases in Central Asia (SKL-HIDCA-2022-DX3, SKL-HIDCA-2021-17), National Natural Science Foundation of China (81960258, 82060589), and China Postdoctoral Science Foundation (2020M670075ZX).

Data availability statement

The datasets generated during and/or analyzed during the current study are available from the corresponding author on reasonable request.

Declaration of competing interest

The authors declare that they have no known competing financial interests or personal relationships that could have appeared to influence the work reported in this paper.

Acknowledgements

We would like to thank State Key Laboratory of Pathogenesis, Prevention and Treatment of High Incidence Diseases in Central Asia, National Natural Science Foundation of China, and China Postdoctoral Science Foundation for the funding support to this study.

We would also like to thank State Key Laboratory of Pathogenesis, Prevention, and Treatment of High Incidence Diseases in Central Asia and Clinical Medical Research Institute of Xinjiang Medical University for providing infrastructure, laboratory space and equipment for experiments.

Appendix A. Supplementary data

Supplementary data to this article can be found online at https://doi.org/10.1016/j.heliyon.2023.e18491.

References

[[1] Global Burden of Disease Collaborators 2013 Global, regional, and national incidence, prevalence, and years lived with disability for 301 acute and chronic diseases and injuries in 188 countries, 1990-2013: a systematic analysis for the Global Burden of Disease Study, Lancet 386 (9995) (2015) 743–800.
[2] R.I. Holt, M. de Groot, I. Lucki, et al., NIDDK international conference report on diabetes and depression: current understanding and future directions, Diabetes Care 37 (8) (2016) 2067–2077.
[3] M. de Groot, K.A. Crick, M. Long, et al., Lifetime duration of depressive disorders in patients with type 2 diabetes, Diabetes Care 39 (12) (2016) 2174–2181.
[4] L. Ducat, L.H. Philipson, B.J. Anderson, The mental health comorbidities of diabetes, JAMA 312 (7) (2014) 691–692.
[5] S. Wild, G. Roglic, A. Green, et al., Global prevalence of diabetes: estimates for the year 2000 and projections for 2030, Diabetes Care 27 (5) (2004) 1047–1053.
[6] T.M. Dall, W. Yang, P. Halder, et al., The economic burden of elevated blood glucose levels in 2012: diagnosed and undiagnosed diabetes, gestational diabetes mellitus, and prediabetes, Diabetes Care 37 (12) (2014) 3172–3179.
[7] M. Deuschle, Effects of antidepressants on glucose metabolism and diabetes mellitus type 2 in adults, Curr. Opin. Psychiatr. 26 (1) (2013) 60–65.
[8] W. Katon, J. Russo, E.H. Lin, et al., Cost-effectiveness of a multicondition collaborative care intervention：a randomized controlled trial, Arch. Gen. Psychiatr. 69 (5) (2012) 506–514.
[9] W.J. Katon, J.E. Russo, S.R. Heckbert, et al., The relationship between changes in depression symptoms and changes in health risk behaviors in patients with diabetes, Int. J. Geriatr. Psychiatr. 25 (5) (2010) 466–475.
[10] J.Y. Chung, J.H. Jeong, J. Song, Resveratrol modulates the gut-brain Axis: focus on glucagon-like peptide-1, 5-HT, and gut microbiota, Front. Aging Neurosci. 12 (2020), 588044.
[11] Chinese Society of Endocrinology, Chinese Diabetes Society, Consensus recommendations on utilizing glucagon-like peptide-1 (GLP-1) receptor agonists in the treatment of type 2 diabetes mellitus Chin, J. Intern. Med. 59 (11) (2020) 836–846.
[12] T.D. Müller, B. Finan, S.R. Bloom, et al., Glucagon-like peptide 1 (GLP-1), Mol. Metabol. 30 (2019) 72–130.
[13] K. Semenkovich, M.E. Brown, D.M. Svrakic, et al., Depression in type 2 diabetes mellitus: prevalence, impact, and treatment, Drugs 75 (6) (2015) 577–587.
[14] J.S. Snyder, A. Soumier, M. Brewer, et al., Adult hippocampal neurogenesis buffers stress responses and depressive behaviour, Nature 476 (7361) (2011) 458–461.
[15] M. Colla, G. Kronenberg, M. Deuschle, et al., Hippocampal volume reduction and HPA-system activity in major depression, J. Psychiatr. Res. 41 (7) (2007) 553–560.
[16] N. Ho, M.S. Sommers, I. Lucki, Effects of diabetes on hippocampal neurogenesis: links to cognition and depression, Neurosci. Biobehav. Rev. 37 (8) (2013) 1346–1362.
[17] S.Q. Han, R.P. Zheng, S.Y. Li, et al., Progressive brain structural abnormality in depression assessed with MR imaging by using causal network analysis, Psychol. Med. 29 (2021) 1–10.
[18] L.P. Zhao, R.F. Liu, Y.S. Lu, et al., Resting-state hippocampal functional connectivity in patients with type 2 diabetes mellitus, Chinese Journal of Medical Imaging 28 (7) (2020) 482–487.
[19] D. Jantas, Cell-based systems of depression: an overview, in: Herbal Medicine in Depression, Springer International Publishing, Cham, Switzerland, 2016, pp. 75–117, 9783319140216.
[20] A.S. Correia, S. Fraga, J.P. Teixeira, et al., Cell model of depression: reduction of cell stress with mirtazapine, Int. J. Mol. Sci. 23 (9) (2022) 4942.
[21] M.R. Akanda, M.J. Kim, I.S. Kim, et al., Neuroprotective effects of sigesbeckia pubescens extract on glutamate-induced oxidative stress in HT22 cells via down regulation of MAPK/caspase-3 pathways, Cell. Mol. Neurobiol. 38 (2) (2018) 497–505.
[22] P. Grant, D. Lipscomb, J. Quin, Psychological and quality of life changes in patients using GLP-1 analogues, J. Diabet. Complicat. 25 (4) (2011) 244–246.
[23] Q. Ma, Q.S. Xu, L.L. Zhang, et al., Correlation between intestinal glucagon-like peptides-1 and major depressive disorder, Chin. J. Behav. Med. Brain. Sci. 31 (3) (2022) 255–260.
[24] A.N. Sharma, S.S. Ligade, J.N. Sharma, et al., GLP-1 receptor agonist liraglutide reverses long-term atypical antipsychotic treatment associated behavioral depression and metabolic abnormalities in rats, Metab. Brain Dis. 30 (2) (2015) 519–527.
[25] J.J. Schildkraut, The catecholamine hypothesis of affective disorders: a review of supporting evidence, J. Neuropsychiatry Clin. Neurosci. 7 (4) (1995) 524–533, 1965.
[26] E.J. Nestler, Antidepressant treatments in the 21st century, Biol. Psychiatr. (4) (1998) 526–533.
[27] O. Berton, E.J. Nestler, New approaches to antidepressant drug discovery: beyond monoamines, Nat. Rev. Neurosci. (7) (2006) 137–151.
[28] M.E. Bach, M. Barad, H. Son, et al., Age -related defects in spatial memory are correlated with defects in the late phase of hippocampal long -term potentiation in vitro and are attenuated by drugs that enhance the cAMP signaling pathway, Proc. Natl. Acad. Sci. U.S.A. 96 (9) (1999) 5280.
[29] M. Motaghinejad, M. Motevalian, S. Fatima, et al., The neuroprotective effect of curcumin against nicotine-induced neurotoxicity is mediated by CREB-BDNF signaling pathway, Neurochem. Res. 42 (2017) 2921–2932.
[30] L.B. Zhao, R. Guo, N.N. Cao, et al., An integrative pharmacology-based pattern to uncover the pharmacological mechanism of ginsenoside H dripping pills in the treatment of depression, Front. Pharmacol. 11 (2020), 590457.
[31] H. Yu, S.M. Shao, J.N. Xu, et al., Persimmon leaf extract alleviates chronic social defeat stress-induced depressive-like behaviors by preventing dendritic spine loss via inhibition of serotonin reuptake in mice, Chin. Med. 17 (2022) 65.
[32] C.A. Saura, J.R. Cardinaux, Emerging roles of CREB-regulated transcription coactivators in brain physiology and pathology, Trends Neurosci. 40 (12) (2017) 720–733.
[33] W.F. Hu, J.J. Wu, T. Ye, et al., Farnesoid X receptor-mediated cytoplasmic translocation of CRTC2 disrupts CREB-BDNF signaling in hippocampal CA1 and leads to the development of depression-like behaviors in mice, Int. J. Neuropsychopharmacol. 23 (2020) 673–686.
[34] Y.S. Ramezany, M. Nourhashemi, S. Keshavarzi, et al., Possible role of cyclic AMP response element binding/brain-derived neurotrophic factor signaling pathway in mediating the pharmacological effects of duloxetine against methamphetamine use-induced cognitive impairment and withdrawal-induced anxiety and depression in rats, Adv. Biomed. Res. 8 (2019) 11.